

# 3 GHz, fundamentally mode-locked, femtosecond Yb-fiber laser

Hung-Wen Chen,<sup>1</sup> Guoqing Chang,<sup>1</sup> Shanhui Xu,<sup>2</sup> Zhongmin Yang,<sup>2,4</sup> and Franz X. Kärtner<sup>1,3,5</sup>

<sup>1</sup>Research Laboratory of Electronics, Massachusetts Institute of Technology, 77 Massachusetts Avenue, Cambridge, Massachusetts 02139, USA

<sup>2</sup>State Key Laboratory of Luminescent Materials and Devices and Institute of Optical Communication Materials, South China University of Technology, Guangzhou 510640, China

<sup>3</sup>Center for Free-Electron Laser Science, DESY and University of Hamburg, Notkestraße 85, 22607 Hamburg, Germany

<sup>4</sup>e-mail: yangzm@scut.edu.cn

<sup>5</sup>e-mail: kaertner@mit.edu

Received June 6, 2012; revised July 13, 2012; accepted July 13, 2012;  
posted July 16, 2012 (Doc. ID 169509); published August 21, 2012

We demonstrate a fundamentally mode-locked Yb-fiber laser with 3 GHz repetition rate and ~206 fs pulse duration. The laser incorporates two enabling technologies: a 1 cm heavily Yb-doped phosphate glass fiber as the gain medium and a high-dispersion (~1300 fs<sup>2</sup>) output coupler to manage cavity dispersion. The oscillator self-starts and generates up to 53 mW average power. © 2012 Optical Society of America

OCIS codes: 140.3510, 060.3510, 140.4050, 140.7090, 320.7090.

High-repetition-rate (>1 GHz) lasers with femtosecond pulse duration are required in many applications. For nonlinear bio-optical imaging (e.g., two-photon fluorescence excitation microscopy), in which photo-induced damage is caused by pulse energy rather than average power, increasing pulse repetition rate will improve signal-to-noise ratio and reduce data acquisition time [1]. Frequency combs, which are achieved by fully stabilizing both the repetition rate and the carrier-envelope offset frequency of multi-GHz lasers, exhibit large line spacing (equal to the laser's repetition rate) that may permit access to and manipulation of each individual comb line. Such capabilities have opened numerous frequency domain applications, including optical arbitrary waveform generation, high-speed analog-to-digital conversion, and high-resolution spectroscopy [2]. Of particular importance is precision calibration of astronomical spectrographs to search for Earth-like exoplanets, which normally requires femtosecond laser frequency combs with >15 GHz line spacing ("astro-comb") [3–8]. Current implementation of an astro-comb relies on using multiple Fabry–Perot (FP) filtering cavities to multiply the line spacing of a frequency comb based on low-repetition-rate lasers. For example, Wilken *et al.*'s astro-comb system employed a 250 MHz Yb-fiber laser as the front end, followed by three cascade FP filtering cavities for line-space multiplication [7]. Stabilizing these FP cavities, locking them to the frequency comb, and preventing parasitic cavities between two FP cavities constitute the major challenge in constructing a practical astro-comb. Such an issue can be alleviated by employing a frequency comb based on a femtosecond laser operating at a much higher repetition rate (e.g., 3–10 GHz). The significantly simplified astro-comb requires only one FP cavity and becomes more reliable.

Several types of femtosecond mode-locked lasers have demonstrated operation with a >1 GHz repetition rate [9–15]. Up to date, however, fully stabilized frequency combs with >1 GHz comb spacing are only implemented based on Ti:Sapphire lasers (10 GHz) [16], Yb-fiber lasers (1 GHz) [17], and most recently Er-fiber lasers

(1 GHz) [18]. Among them, Yb-fiber laser frequency combs possess superior power scalability thanks to the rapid development of double-clad Yb-fibers and high-brightness pump diodes, as well as the Yb-fiber's high pump-to-signal conversion efficiency (~80%). For example, Yb-fiber laser frequency combs with 80 W average power have been demonstrated, albeit at a lower repetition rate of 154 MHz [19]. Such power scalability is critical for multi-GHz frequency combs involved in nonlinear optical applications (e.g., wavelength conversion into visible wavelength range), in which pulse energies of several nanojoules are nominally required.

Constructing fundamentally mode-locked Yb-fiber lasers with a >1 GHz repetition rate and femtosecond pulse duration demands two crucial elements: (1) a short (<10 cm), highly doped Yb-fiber to provide enough round-trip gain and self-phase modulation, and (2) a dispersion compensating device to provide enough negative group delay dispersion (GDD) to compensate for the positive GDD from the Yb-fiber and other intracavity components (e.g., lens). A laser cavity with a net negative GDD is necessary to ensure soliton-like pulse formation that serves as the main pulse-shortening mechanism for high-repetition-rate fiber lasers to generate femtosecond pulses [20]. Recently, Ingmar Hartl *et al.* demonstrated 1.04 GHz Yb-fiber lasers (fully stabilized) using 6 cm gain fiber spliced to a fiber Bragg grating for dispersion compensation [17]. By further shortening the gain fiber (down to 4 cm) and employing a Martinez compressor for dispersion compensation, the same group has increased the repetition rate up to 1.6 GHz [14]. Further repetition rate scaling apparently demands shrinking the laser cavity by shortening the gain fiber and avoiding a bulky free-space device (e.g., diffraction grating) for dispersion compensation. Here we present a 3 GHz femtosecond Yb-fiber laser incorporating two key technologies: (1) a 1 cm, heavily Yb-doped phosphate glass fiber as the gain medium and (2) a high-dispersion output coupler for dispersion compensation.

As shown in Fig. 1, the laser is configured as a linear cavity (indicated by the red dashed circle) with a total

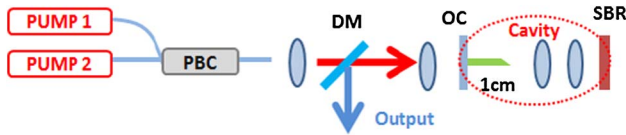


Fig. 1. (Color online) Schematic setup of the 3 GHz Yb-fiber oscillator. PBC, polarization beam combiner; DM, dichroic mirror; OC, output coupler; and SBR, saturable Bragg reflector.

length of  $\sim 4.2$  cm. Two fiber-coupled pump diodes are power combined using a polarization beam combiner, providing up to 1.2 W of average power centered at 976 nm. A dichroic mirror inserted between the combiner and the laser cavity separates the output laser power from the pump. The gain is provided by 1 cm Yb-doped phosphate glass fiber, which has the highest reported  $\text{Yb}^{3+}$  concentration of 15.2 wt. % and exhibits 46 dB/cm of absorption at 976 nm. The measured net gain coefficient of the phosphate glass fiber was 5.7 dB/cm [21]. Other important parameters are 1.84 ms upper-state lifetime,  $5 \mu\text{m}$  core diameter, and numerical aperture of 0.14. The fiber is encapsulated in a 1 cm ceramic ferrule held by a specially designed strain relief clamp. Due to the large surface-to-volume ratio for the fiber, the resulting intrinsically efficient heat dissipation requires no extra cooling. During the experiments, thermal damage of the fiber is absent. The straight cleaved end of the fiber is directly attached to an output coupler that transmits  $>98\%$  of the 976 nm pump and reflects  $\sim 95\%$  of the lasing power. Fine adjustment is necessary to eliminate possible air gaps between the output coupler and the fiber end. Any noticeable etalon effect might prevent the laser from mode locking.

The specially designed coating on the output coupler provides  $-1300 \text{ fs}^2$  GDD at  $1.025 \mu\text{m}$ , enough to render a negative-dispersion laser cavity for soliton pulse formation. The thickness of the coating is  $\sim 10 \mu\text{m}$ , with alternative layers of  $\text{Ta}_2\text{O}_5$  and  $\text{SiO}_2$ . The reflectivity between 1010 nm and 1040 nm is within the range of 94%–96%. The other end of the Yb-fiber is angle ( $\sim 8^\circ$ ) cleaved to avoid back reflection. Two aspheric lenses re-image the fiber output onto a saturable absorber reflector (SBR) to initialize the mode locking. The commercially available SBR (from BATOP, model: SAM-1040-8-1ps) has a modulation depth of 5%, a saturation fluence of  $40 \mu\text{J}/\text{cm}^2$ , and recovery time of 1 ps. The spot size on the SBR is  $\sim 13 \mu\text{m}$  in diameter.

The dependence of output power on the input pump power is illustrated in Fig. 2 for different operation regimes. At relatively low pump power, the oscillator operates at continuous wave mode. Mode locking self-starts as the pump power reaches  $\sim 800$  mW. Increasing the pump power from 800 mW to 1.15 W, the mode-locked output power grows accordingly from 32 mW to 53 mW.

We characterized the laser at 1073 mW input pump power, corresponding to a laser power of 49 mW. The measured optical spectrum, shown in Fig. 3(a), has a 5.5 nm bandwidth at full width at half maximum (FWHM). The RF spectrum recorded in the inset of Fig. 3(a) indicates a 3 GHz repetition rate with a signal-to-background ratio  $>60$  dB. The output pulses are also measured using an autocorrelator; the resulting autocorrelation trace plotted in Fig. 3(b) shows a 319 fs

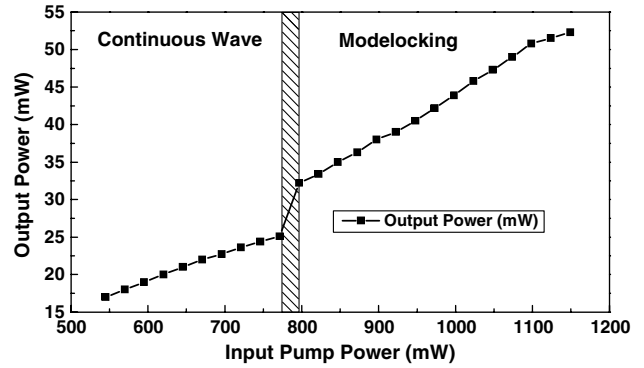


Fig. 2. Output power versus input pump power. Mode locking self-starts as the input pump power exceeds 800 mW.

FWHM duration (solid curve). As a comparison, the auto-correlation trace of the transform-limited pulse calculated from the optical spectrum in Fig. 3(a) is plotted in Fig. 3(b) as the red dashed curve. With a deconvolution factor of 1.54 (assuming a hyperbolic secant pulse profile), the pulse duration is estimated to be  $\sim 206$  fs. It is about 56 fs longer than the transform-limited duration (i.e., 150 fs), showing that the optical pulses are slightly chirped.

Without any enclosure of the laser or any other means to prevent ambient disturbance (e.g., air current, vibration, temperature fluctuation), we measured the relative intensity noise (RIN) of the 3 GHz laser running at the input pump power of 1073 mW, shown as the blue curve

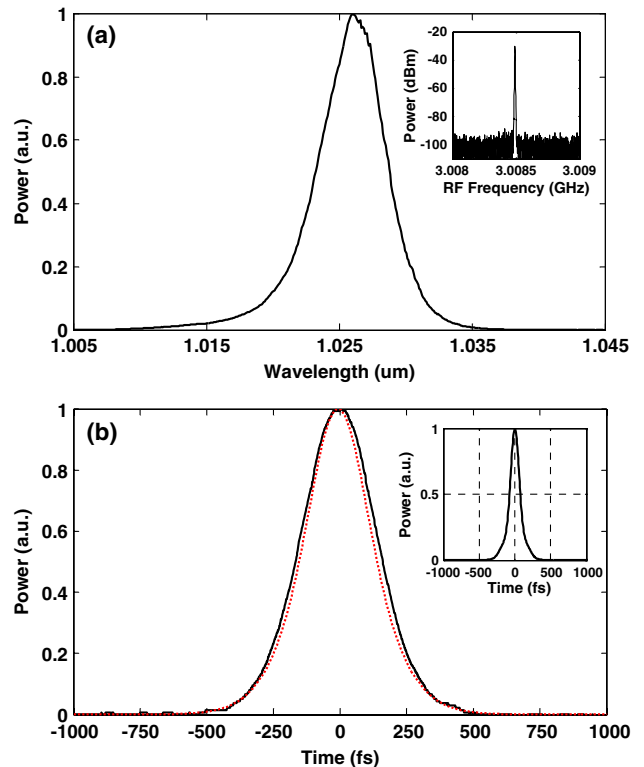


Fig. 3. (Color online) (a) Optical spectrum of the output pulse with 1073 mW pump power. Inset: RF spectrum with a resolution bandwidth of 3 kHz. (b) Measured autocorrelation trace of the output pulse (solid curve) and the calculated autocorrelation trace of the transform-limited pulse (red dashed curve). Inset: transform-limited pulse.

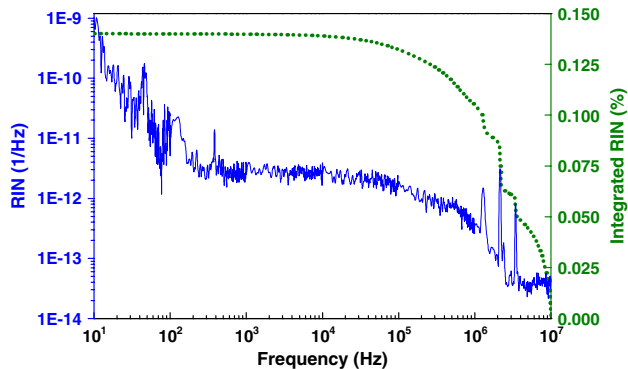


Fig. 4. (Color online) Relative intensity noise (RIN) (blue curve) of the mode-locked 3 GHz Yb-fiber laser and the integrated RIN (green dashed curve).

in Fig. 4. Also plotted in the same figure (green dashed curve) is the integrated RIN. Integration between 10 Hz and 10 MHz results in an integrated RIN of 0.14%.

In conclusion, we have demonstrated a fundamentally mode-locked, femtosecond ( $\sim 206$  fs) Yb-fiber laser with, to the best of our knowledge, the highest repetition rate of 3 GHz among reported femtosecond Yb-fiber lasers. With 1 cm heavily Yb-doped phosphate glass fiber as the gain medium and a high-dispersion ( $-1300$  fs<sup>2</sup>) output coupler for dispersion compensation, the laser self-starts and produces up to 53 mW of average power. The mode locking usually lasts about three days, until the focusing spot on the SBR is damaged. Shifting to a different spot immediately recovers the mode locking. Use of a back-thinned SBR facilitates heat dissipation and prevents thermal damage. With this method, the mode locking has lasted for 30 days and counting. No SBR damage occurs. The current intracavity loss is estimated to be  $\sim 50\%$ , which allows us to use an output coupler with larger output coupling ratio (e.g., 10%) to increase the output power (and thus the power efficiency) of the laser without losing the mode locking. Ongoing work includes further repetition rate scaling up to 10 GHz by directly sandwiching the 1 cm Yb-fiber between the output coupler and the SBR while maintaining femtosecond pulse duration. Meanwhile, we are working on stabilizing both the repetition rate and the carrier-envelope offset frequency of the current laser to achieve a frequency comb with 3 GHz line spacing.

This work was supported under National Aeronautics and Space Administration (NASA) grants NNX10AE68G, NNX09AC92G and National Science Foundation (NSF) grants AST-0905592 and AST-1006507. The authors thank Duo Li for his help with noise measurements.

## References

1. N. Ji, J. C. Magee, and E. Betzig, *Nat. Methods* **5**, 197 (2008).
2. S. A. Diddams, *J. Opt. Soc. Am. B* **27**, B51 (2010).
3. C.-H. Li, A. J. Benedick, P. Fendel, A. G. Glenday, F. X. Kärtner, D. F. Phillips, D. Sasselov, A. Szentgyorgyi, and R. L. Walsworth, *Nature* **452**, 610 (2008).
4. T. Steinmetz, T. Wilken, C. Araujo-Hauck, R. Holzwarth, T. W. Hänsch, L. Pasquini, A. Manescau, S. D'Odorico, M. T. Murphy, T. Kentischer, W. Schmidt, and T. Udem, *Science* **321**, 1335 (2008).
5. D. A. Braje, M. S. Kirchner, S. Osterman, T. Fortier, and S. A. Diddams, *Eur. Phys. J. D* **48**, 57 (2008).
6. G. Chang, C.-H. Li, D. F. Phillips, R. L. Walsworth, and F. X. Kärtner, *Opt. Express* **18**, 12736 (2010).
7. T. Wilken, G. L. Curto, R. A. Probst, T. Steinmetz, A. Manescau, L. Pasquini, J. I. G. Hernández, R. Rebolo, T. W. Hänsch, T. Udem, and R. Holzwarth, *Nature* **485**, 611 (2012).
8. G. G. Ycas, F. Quinlan, S. A. Diddams, S. Osterman, S. Mahadevan, S. Redman, R. Terrien, L. Ramsey, C. F. Bender, B. Botzer, and S. Sigurdsson, *Opt. Express* **20**, 6631 (2012).
9. A. Bartels, D. Heinecke, and S. A. Diddams, *Opt. Lett.* **33**, 1905 (2008).
10. D. Li, U. Demirbas, J. R. Birge, G. S. Petrich, L. A. Kolodziejski, A. Sennaroglu, F. X. Kärtner, and J. G. Fujimoto, *Opt. Lett.* **35**, 1446 (2010).
11. S. Yamazoe, M. Katou, T. Adachi, and T. Kasamatsu, *Opt. Lett.* **35**, 748 (2010).
12. S. Pekarek, A. Klenner, T. Südmeyer, C. Fiebig, K. Paschke, G. Erbert, and U. Keller, *Opt. Express* **20**, 4248 (2012).
13. J. Chen, J. W. Sickler, H. Byun, E. P. Ippen, S. Jiang, and F. X. Kärtner, in *Ultrafast Phenomena XVI*, P. Corkum, S. Silvestri, K. A. Nelson, E. Riedle, R. W. Schoenlein, F. P. Schäfer, J. P. Toennies, and W. Zinth, eds. (Springer, 2009), pp. 732–734.
14. I. Hartl, A. Romann, and M. E. Fermann, in *2011 Conference on Lasers and Electro-Optics* (Optical Society of America, 2011), pp. 1–2.
15. M. Endo, A. Ozawa, and Y. Kobayashi, *Opt. Express* **20**, 12191 (2012).
16. A. Bartels, D. Heinecke, and S. A. Diddams, *Science* **326**, 681 (2009).
17. I. Hartl, H. A. McKay, R. Thapa, B. K. Thomas, L. Dong, and M. E. Fermann, in *Conference on Lasers and Electro-Optics/International Quantum Electronics Conference* (Optical Society of America, 2009), paper CMN1.
18. D. Chao, M. Sander, G. Chang, J. Morse, J. Cox, G. Petrich, L. Kolodziejski, F. Kaertner, and E. Ippen, in *Optical Fiber Communication Conference* (Optical Society of America, 2012), paper OW1C.2.
19. A. Ruehl, A. Marcinkevicius, M. E. Fermann, and I. Hartl, *Opt. Lett.* **35**, 3015 (2010).
20. D. Pudo, H. Byun, J. Chen, J. Sickler, F. X. Kärtner, and E. P. Ippen, *Opt. Express* **16**, 19221 (2008).
21. S. Xu, Z. Yang, W. Zhang, X. Wei, Q. Qian, D. Chen, Q. Zhang, S. Shen, M. Peng, and J. Qiu, *Opt. Lett.* **36**, 3708 (2011).